Bol. Soc. Paran. Mat.
©SPM – E-ISSN-2175-1188
SPM: www.spm.uem.br/bspm

(3s.) **v. 2026 (44) 12** : 1–24.
ISSN-0037-8712
doi:10.5269/bspm.83015

Mathematical Formalization of Indian Medical Heritage: A Novel TB Model with Āyurveda-Inspired Behavioral Adoption Dynamics

[1]Harshita Kaushik, [2]Prashant Upadhyaya, [3]Ruchika Singh

ABSTRACT: Tuberculosis remains a critical public health challenge in India, where traditional knowledge systems offer culturally embedded preventive practices. Formal integration of such knowledge into epidemiological models can enhance intervention strategies. We develop a novel deterministic compartmental model incorporating principles from Indian Knowledge Systems (IKS). The model extends classical TB epidemiology with dual latent compartments, reinfection, treatment staging, and a behavioral adoption component representing IKS practice uptake. Mathematical analysis includes well-posedness proofs, derivation of the basic reproduction number R_0, equilibrium characterization, stability analysis, and sensitivity assessment. The model exhibits backward bifurcation at $R_0 = 1$, with the disease-free equilibrium being globally asymptotically stable when $R_0 < 1$ and the endemic equilibrium globally stable when $R_0 > 1$. Sensitivity analysis identifies IKS efficacy (ε_S) and adoption parameters (μ_a, κ_a) as key factors reducing R_0. Numerical simulations demonstrate that IKS adoption flattens infection curves and modifies long-term disease dynamics. This study provides the first mathematical formalization of IKS principles in epidemiological modeling, offering a culturally contextualized framework for TB control policy and establishing a methodology for integrating traditional knowledge systems into computational public health.

Keywords: Tuberculosis modeling, Indian Knowledge Systems, epidemiological dynamics, behavioral adoption, cultural epidemiology.

Contents

2020 *Mathematics Subject Classification:* 93D05, 93C15, 92-08.
Submitted March 26, 2026. Published June 09, 2026.

1. Introduction

Tuberculosis (TB), a pandemic driven by Mycobacterium tuberculosis, remains a critical global health challenge. The World Health Organization (WHO) estimates 10.6 million new cases and 1.3 million deaths annually, with the shadow of drug-resistant (MDR/RR-TB and XDR-TB) strains looming large [1]. In the fight against such a complex pathogen, mathematical modelling has become a cornerstone of public health strategy, offering a quantitative framework to simulate disease spread, predict outbreak trajectories, and evaluate the efficacy of control measures like vaccination and case-finding [2]. The Susceptible-Exposed-Infectious-Recovered (SEIR) model and its derivatives have been particularly influential in capturing the unique latency and reactivation dynamics of TB [3].

However, a significant limitation of these conventional models is their focus on broad epidemiological compartments, often overlooking the intricate physiological and metabolic host factors that determine an individual's journey from infection to active disease. A paradigm that incorporates these host-level determinants of susceptibility and progression could yield more granular, predictive, and personally relevant models.

Strikingly, this need for a holistic, systems-level understanding finds a profound echo in the ancient Indian medical science of Ayurveda. The disease known as Rajayakshma or Shosha is described with a clinical precision that encompasses not just symptoms but a complete etiopathological framework. The foundational shloka on its etiology states:

"Malajalagatiroddhānmaithunādvā vighātāt |
Darśanavirastabhāvācchleṣmaroddhātsaṃsṛjāṃ ca ||
Kupitaskaladoṣairvyāptadehasya jaṃtostu | Bhavati viṣamaśothavyādhireṣātikṛcchraḥ ||"

This translates to the disease arising from factors including the suppression of natural urges (e.g., stool, urine), excessive sexual activity, physical trauma, consumption of incompatible or excessively heavy and sweet foods, and the obstruction of Kapha (phlegm) in the body's channels. When the bodily humors (Doshas—Vata, Pitta, Kapha) become collectively vitiated and pervade the entire system, the dreadful wasting disease Shosha manifests, which is exceedingly difficult to treat [4, 5].

This framework aligns with modern science. The suppression of natural urges and physical trauma can be interpreted as physiological stressors that compromise immunity. A diet imbalanced towards heavy, sweet foods could correlate with dysbiosis and metabolic syndrome, known risk factors for TB progression [6]. The concept of systemic Dosha vitiation mirrors the widespread immune dysregulation and inflammatory cascade seen in active TB [7].

Ayurveda's sophistication is further evidenced by its detailed description of premonitory signs (Purvarupa), which signal the disease's onset before its full manifestation:

"Bahuvimalakaphātiśvāsaviśvāṅgasādaḥ | Vamanagalaviṣopāstyannamādyonmadāśca ||
Dhavalannayānatā nidrātiḥ sa pīnasatvaṃ ca | Bhavati hi khalu śoṣe pūrvaṃ rūpāṇi tāni ||"

The symptoms include: profuse, clear phlegm, severe dyspnea, generalized weakness or debility, vomiting, a burning sensation in the throat, indigestion and loss of appetite, mental confusion, whiteness of the eyes, excessive sleep, and nasal discharge [4, 5]. This prodromal phase represents a critical window where the host's system is beginning to fail, moving from a state of balance to one of pathology.

The text then elaborates on the fully manifested symptoms (Rupa), providing a stark picture of the advanced disease:

"Pārśvakṛśatākārṣṇyaṃ bhaṅgasvarabhedanāṅga | Śuṣkatākṣitvaṃ kāsasvaraḥ pārśvaśūlaṃ daḥṣṭiḥ ||
Jṛmbhaṇāṅgamardatṛṣṇācchardikāyāḥ pravṛttiḥ | Kaphasya copaśāntiśca śvayathuḥ sarvagātrajaḥ ||"

This describes emaciation of the flanks, blackish discoloration, a broken voice, body pain, dryness, wasting, cough, hoarseness of voice, pain in the flanks, a burning sensation, yawning, body aches, thirst, vomiting, and the subsidence of Kapha, followed by generalized swelling over the entire body [4, 5]. This

progression—from respiratory and digestive disturbances to systemic wasting, cachexia, and ultimately multi-organ involvement—provides a dynamic, stage-based clinical picture that is absent from standard SEIR models.

The text concludes with a crucial shloka that provides a diagnostic and prognostic quantification, a concept highly relevant to mathematical modeling:

"Pārśvakṛśatākārṣṇyannaṣṭabhaṅgasvarabhedanāṅga | Śuṣkatākṣitvaṃ kāsasvaraḥ pārśvaśūlaṃ daḥṣṭiḥ ||
, Jṛmbhaṇāṅgamardatṛṣṇācchardikāyāḥ pravṛttiḥ | Kaphasya copaśāntiśca śvayathuḥ sarvagātrajaḥ ||
Itidaśabhirathai kādhikayā kriyā | Parihāsyastvathī pañcaṣaḍabhiḥ svarūpaiḥ ||"

This states that the disease is diagnosed by the presence of these ten or more symptoms, and that a patient can only be managed, not easily cured, when the disease is fully established with five or six primary symptoms [4, 5]. This quantifiable approach to diagnosis based on symptom clusters is a primitive yet insightful form of clinical scoring and staging. Moreover, the burden of TB in India is marked by pronounced geographical heterogeneity, with states such as Uttar Pradesh, Maharashtra, and Madhya Pradesh reporting disproportionately high incidence rates compared to others. This spatial variation is influenced not only by demographic and socioeconomic factors but also by regional differences in cultural practices and traditional health-seeking behaviours. In areas where Ayurveda and local wellness traditions are deeply embedded, the potential for preventive behavioural adoption may be greater. A geographical perspective, therefore, enriches our understanding of how culturally grounded interventions like IKS can be tailored to regional epidemiological and sociocultural contexts, enhancing the relevance and impact of model-based policy recommendations. It suggests a threshold effect a critical number of pathological manifestations beyond which the disease becomes entrenched and recovery exponentially more difficult. This aligns with modern concepts of disease severity indices and tipping points in complex physiological systems.

Recent research has begun to validate the synergy between traditional knowledge and modern science. Studies have explored the immunomodulatory potential of Ayurvedic formulations [8], and the concept of impaired digestion and metabolism (Agnimandya) has been correlated with mitochondrial dysfunction [9], a key feature in the immunometabolism of TB [10].

Novelty of the work

This paper bridges this historical divide by proposing a novel, multi-compartmental mathematical model for Tuberculosis that formally integrates the principles of the Indian Knowledge System (IKS). The model extends the classic epidemiological structure through two key innovations. First, it includes a vaccination compartment (V) that acknowledges the importance of waning immunity, especially in the elderly, by modeling individuals protected by vaccination with a specific vaccine efficacy (ε_S) and a waning rate (ω_V). Second, and central to this integration, is the modeling of population-level adoption of Ayurvedic preventive practices (x) as a dynamic variable that evolves via a logistic growth equation. This adoption is influenced by the perceived benefit of the practice $B(x)$—which itself is a function of disease prevalence (I/N)—and its cost (C). The uptake of these practices directly reduces the force of infection by modifying the susceptibility of individuals in the susceptible (S) and vaccinated (V) compartments through the term $\phi(x) = \mu_a + \kappa_a x$. Thus, the model defined by the system of equations captures not only the biological transmission of TB but also the behavioral adaptation of the population based on traditional health wisdom. The primary objectives of this study are: to formulate the novel TB model with IKS integration and establish its mathematical well-posedness by proving the existence, uniqueness, positivity, and boundedness of solutions; to derive the basic reproduction number (R_0) and perform a comprehensive stability analysis of both the Disease-Free and Endemic Equilibrium points; to rigorously analyze the global stability of these equilibria using Lyapunov functions and LaSalle's Invariance Principle; and to demonstrate, through mathematical formalism, how the incorporation of IKS, by reducing host susceptibility, can lower R_0 and contribute to the global stability of the disease-free state, offering a quantifiable framework for integrating traditional knowledge into modern public health strategy.

2. Model Description

In this paper, we develop a deterministic compartmental model for tuberculosis (TB) transmission dynamics incorporating behavioral adoption of Indian Knowledge Systems (IKS) practices. The model assumes homogeneous mixing of individuals within an elderly population under consideration. To formulate the model, we have divided the total population into mutually exclusive epidemiological states based on their TB infection status and preventive behavior adoption. Here, we denote the susceptible population by $S(t)$, the population adopting IKS/vaccination by $V(t)$, the exposed population (infected but not yet infectious) by $E(t)$, the latently infected population with high progression rate by $L_f(t)$, the latently infected population with low progression rate by $L_s(t)$, the infectious population with active TB by $I(t)$, the diagnosed population under treatment by $D(t)$, and the recovered population by $R(t)$. Additionally, we track the proportion of population adopting IKS practices as $x(t)$.

The total population $N(t)$ at any time t is the sum of all epidemiological compartments:

$$N(t) = S(t) + V(t) + E(t) + L_f(t) + L_s(t) + I(t) + D(t) + R(t).$$

A schematic representation of the compartmental model is shown in Figure 2.

In the proposed model, susceptible individuals enter the population at a constant recruitment rate Λ. The force of TB infection is

$$\lambda(t) = \frac{\beta}{N}(I + \eta_D D),$$

where β is the transmission coefficient and η_D is the relative infectivity of diagnosed individuals. Susceptible individuals can adopt IKS practices at rate

$$\phi(x) = \mu_a + \kappa_a x,$$

where μ_a is the base adoption rate and κ_a is the social influence factor. IKS adopters experience reduced susceptibility with efficacy ε_S, resulting in force of infection

$$\lambda_V = (1 - \varepsilon_S)\lambda.$$

Exposed individuals progress to either fast latent (L_f) or slow latent (L_s) compartments at rates $p\gamma$ and $(1-p)\gamma$ respectively, where γ is the progression rate and p is the proportion progressing to fast latency. Latent individuals reactivate to active TB at rates κ_f (fast) and κ_s (slow). Infectious individuals are diagnosed at rate δ, and diagnosed individuals receive treatment at rate τ. Successful treatment leads to recovery at rate $\sigma\tau$, where σ is the treatment success proportion. Recovered individuals experience partial immunity with susceptibility factor ρ_R, resulting in force of infection

$$\lambda_R = \rho_R \lambda,$$

and may relapse to latent infection at rate α_R.

The behavioral adoption dynamics follow evolutionary game theory, where the proportion of IKS adopters $x(t)$ evolves according to

$$\dot{x}(t) = vx(1-x)(B(x) - C),$$

where v is the adaptation speed, $B(x) = b_0 + b_1(I/N)$ is the benefit function, and C is the adoption cost. Natural mortality occurs at rate μ in all compartments, with additional TB-induced mortality μ_T for infectious individuals. All model parameters are non-negative and their descriptions with baseline values are provided in Table 1. Although the model is formulated under the assumption of a homogeneous population, the parameters can be interpreted in a **spatially explicit manner**. For instance, the base adoption rate μ_a may reflect regional differences in baseline engagement with Ayurvedic practices, which tend to be stronger in states like Kerala, Uttarakhand, and certain parts of northern India. Similarly, the social influence factor κ_a could capture the effect of community networks, which vary between dense urban settlements and dispersed rural communities. The efficacy parameter ε_S might also depend on local environmental factors, dietary habits, and accessibility to traditional health resources. This spatial

interpretability of parameters lays the groundwork for future extensions into geographically stratified or meta-population frameworks. The model incorporates key features of TB epidemiology including dual latency, reinfection, treatment staging, and behavioral feedback through IKS adoption, providing a comprehensive framework to study TB dynamics in cultural context.

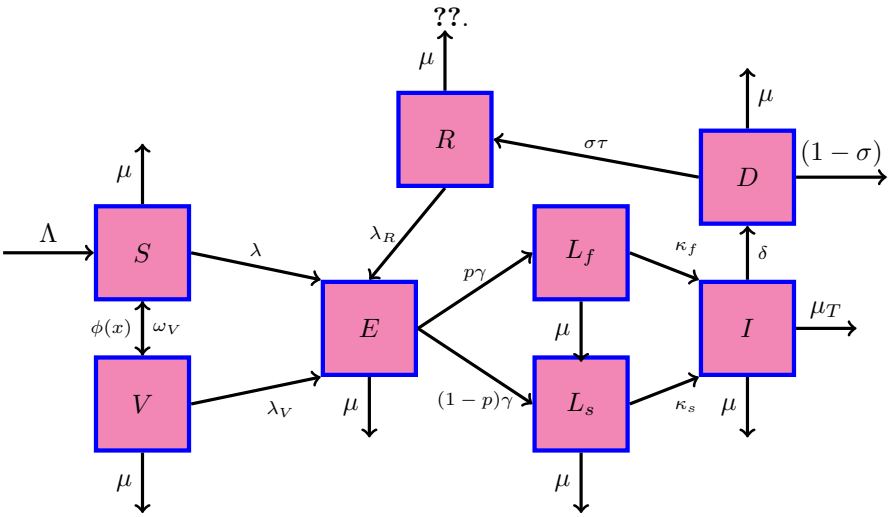

Figure 1: Compartmental Diagram of the model

The Model is as follows :

$$\begin{cases} \dot{S}(t) = \Lambda - \lambda S - \phi(x)S + \omega_V V - \mu_h S \\ \dot{V}(t) = \phi(x)S - \lambda_V V - \omega_V V - \mu V \\ \dot{E}(t) = \lambda S + \lambda_V V + \lambda_R R - (\gamma + \mu)E \\ \dot{L_f}(t) = p\gamma E - (\kappa_f + \mu)L_f \\ \dot{L_s}(t) = (1-p)\gamma E - (\kappa_s + \mu)L_s \\ \dot{I}(t) = \kappa_f L_f + \kappa_s L_s - (\delta + \mu + \mu_T)I \\ \dot{D}(t) = \delta I - (\tau + \mu)D \\ \dot{R}(t) = \sigma\tau D - (\alpha_R + \lambda_R + \mu)R \\ \dot{x}(t) = vx(1-x)(B(x) - C) \end{cases} \tag{2.1}$$

where $\lambda(t) = \dfrac{\beta}{N}(I + \eta_D D), \lambda_V = (1-\varepsilon_s)\lambda, \lambda_R = \rho_R\lambda, \phi(x) = \mu_a + \kappa_a x, B(x) = b_0 + b_1\left(\dfrac{I}{N}\right)$. with all of the parameters being describes in the table below.

Table 1: Parameter Values

Parameter	Description	Value	Source
Λ	Recruitment Rate	1000	Assumed
μ	Natural mortality rate	0.02	India life tables, 2023
β	Transmission rate	12.0	Estimated from TB incidence data, India
γ	Progression rate from E to L	0.5	Tiemersma et al. (2011)
τ	Treatment initiation rate	1.0	India TB Programme Reports
δ	Detection rate	2.0	India TB Programme Reports
σ	Treatment success proportion	0.85	WHO Global TB Report (2023)
η_D	Relative infectivity of D	0.5	Salje et al. (2014)
κ_f	Progression rate from L_f to I	0.1	Vynnycky & Fine (1997)
κ_s	Progression rate from L_s to I	0.01	Sutherland et al. (1982)
μ_T	TB induced mortality rate	0.1	TB mortality statistics, India
α_R	Relapse rate from R	0.05	Menzies et al. (2009)
μ_a	Base IKS adoption rate	0.1	Assumed
κ_a	IKS adoption scaling factor	0.5	Assumed
ω_V	Waning vaccine immunity rate	0.1	TB vaccine literature
ε_S	IKS efficacy	0.6	Assumed for model analysis
ρ_R	Susceptiblity factor for R	0.5	Estimated from reinfection studies
p	Fast latency proportion	0.3	Styblo (1991)
b_0	Base benefit of IKS	0.8	Assumed
b_1	IKS benefit scaling with prevalence	0.5	Assumed
C	Cost of IKS adoption	0.5	Assumed

3. Properties of the Mathematical Model

We have four properties of the mathematical that we want to prove so that we can ensure existence, uniqueness, boundedness and invariance of the solution.

3.1. Existence and Uniqueness of the Solution

Consider the general form of a first order ODE :

$$\dot{x} = f(t, x), x(t_0) = x_0 \tag{3.1}$$

Theorem 3.1. ***(Uniqueness of Solution)*** *Let D be the domain defined by :*

$$|t - t_0| \leq a, ||x - x_0|| \leq b, x = (x_1, x_2, ..., x_n), x_0 = (x_{10}, x_{20}, ..., x_{n0}) \tag{3.2}$$

and suppose that a function $f(t, x)$ satisfies the Lipschitz condition :

$$||f(t, x_1) - f(t, x_2)|| \leq L||x_1 - x_2||, \text{ where } L \geq 0 \tag{3.3}$$

whenever $(t, x_1), (t, x_2)$ belong to D. Then $\exists\ \delta > 0$ such that there is a unique continuous vector solution $x(t)$ of the system (3.1) in the interval $|t - t_0| \leq \delta$

Lemma 3.1. *If $f(t, x)$ has a continuous partial derivative $\frac{\partial f_i}{\partial x_j}, (\text{where} i, j = 1, 2, ..., n)$ on a bounded convex domain $\mathbb{R}$, where $\mathbb{R}$ denotes the set of real numbers, then it satisfies the Lipschitz condition in $\mathbb{R}$. We look for a bounded solution of the form $0 < \mathbb{R} < \infty$.*

Theorem 3.2. ***(Existence of Solution)***
Let D denote the domain defined in (3.2) such that (3.3) holds. Then there exists a solution of model of system of equations (2.1) - (3.12) which is bounded in the domain D

Proof. Let :

$$f_1 = \Lambda - \lambda S - \phi(x) - \omega_v - \mu_h S \tag{3.4}$$
$$f_2 = \phi(x)S - \lambda_V V - \omega_v V - \mu V \tag{3.5}$$
$$f_3 = \lambda S + \lambda_V V + \lambda_R - (\gamma + \mu)E \tag{3.6}$$
$$f_4 = p\gamma E - (\kappa_f + \mu)L_f \tag{3.7}$$
$$f_5 = (1-p)\gamma E - (\kappa_s + \mu)L_s \tag{3.8}$$
$$f_6 = \kappa_f L_f + \kappa_s L_s - (\delta + \mu + \mu_T)I \tag{3.9}$$
$$f_7 = \delta I - (\tau + \mu)D \tag{3.10}$$
$$f_8 = \sigma\tau D - (\alpha_R + \lambda_R + \mu)R \tag{3.11}$$
$$f_9 = vx(1-x)(B(x) - C) \tag{3.12}$$

We want to show that $\frac{\partial f_i}{\partial x_j}(i, j = 1, 2, ..., 9)$ are continuous and bounded. We present all non-zero partial derivatives

$$\frac{\partial f_1}{\partial x_1} = -\mu_a - \kappa_a x(t) - \frac{\beta(\eta_D D(t) + I(t))}{N} - \mu < \infty,$$
$$\frac{\partial f_1}{\partial x_2} = \omega_V < \infty,$$
$$\frac{\partial f_1}{\partial x_6} = -\frac{\beta S(t)}{N} < \infty,$$
$$\frac{\partial f_1}{\partial x_7} = -\frac{\beta\eta_D S(t)}{N} < \infty,$$
$$\frac{\partial f_1}{\partial x_9} = -\kappa_a S(t) < \infty,$$
$$\frac{\partial f_2}{\partial x_1} = \mu_a + \kappa_a x(t) < \infty,$$
$$\frac{\partial f_2}{\partial x_2} = -\frac{\beta(1-\varepsilon_S)(\eta_D D(t) + I(t))}{N} - \mu - \omega_V < \infty,$$
$$\frac{\partial f_2}{\partial x_6} = -\frac{\beta(1-\varepsilon_S)V(t)}{N} < \infty,$$
$$\frac{\partial f_2}{\partial x_7} = -\frac{\beta\eta_D(1-\varepsilon_S)V(t)}{N} < \infty,$$
$$\frac{\partial f_2}{\partial x_9} = \kappa_a S(t) < \infty,$$
$$\frac{\partial f_3}{\partial x_1} = \frac{\beta(\eta_D D(t) + I(t))}{N} < \infty,$$
$$\frac{\partial f_3}{\partial x_2} = \frac{\beta(1-\varepsilon_S)(\eta_D D(t) + I(t))}{N} < \infty,$$
$$\frac{\partial f_3}{\partial x_3} = -\gamma - \mu < \infty,$$
$$\frac{\partial f_3}{\partial x_6} = \frac{\beta S(t)}{N} + \frac{\beta(1-\varepsilon_S)V(t)}{N} + \frac{\beta\rho_R R(t)}{N} < \infty,$$
$$\frac{\partial f_3}{\partial x_7} = \frac{\beta\eta_D S(t)}{N} + \frac{\beta\eta_D(1-\varepsilon_S)V(t)}{N} + \frac{\beta\eta_D\rho_R R(t)}{N} < \infty,$$

$$\frac{\partial f_3}{\partial x_8} = \frac{\beta\rho_R(\eta_D D(t) + I(t))}{N} < \infty,$$
$$\frac{\partial f_4}{\partial x_3} = \gamma p < \infty,$$
$$\frac{\partial f_4}{\partial x_4} = -\kappa_f - \mu < \infty,$$
$$\frac{\partial f_4}{\partial x_8} = \alpha_R < \infty,$$
$$\frac{\partial f_5}{\partial x_3} = \gamma(1-p) < \infty,$$
$$\frac{\partial f_5}{\partial x_5} = -\mu - \kappa_s < \infty,$$
$$\frac{\partial f_6}{\partial x_4} = \kappa_f < \infty,$$
$$\frac{\partial f_6}{\partial x_5} = \kappa_s < \infty,$$
$$\frac{\partial f_6}{\partial x_6} = -\delta - \mu - \mu_T + \frac{\beta\rho_R^2 R(t)}{N} < \infty,$$
$$\frac{\partial f_6}{\partial x_7} = \frac{\beta\eta_D\rho_R^2 R(t)}{N} < \infty,$$
$$\frac{\partial f_6}{\partial x_8} = \frac{\beta\rho_R^2(\eta_D D(t) + I(t))}{N} < \infty,$$
$$\frac{\partial f_7}{\partial x_6} = \delta < \infty,$$
$$\frac{\partial f_7}{\partial x_7} = -\mu - \tau < \infty,$$
$$\frac{\partial f_8}{\partial x_6} = -\frac{\beta\rho_R R(t)}{N} < \infty,$$
$$\frac{\partial f_8}{\partial x_7} = \sigma\tau - \frac{\beta\eta_D\rho_R R(t)}{N} < \infty,$$
$$\frac{\partial f_8}{\partial x_8} = -\frac{\beta\rho_R(\eta_D D(t) + I(t))}{N} - \mu - \alpha_R < \infty,$$
$$\frac{\partial f_9}{\partial x_6} = \frac{b_1 v(1-x(t))x(t)}{N} < \infty,$$
$$\frac{\partial f_9}{\partial x_9} = v(1-x(t))\left(\frac{b_1 I(t)}{N} + b_0 - c\right) - vx(t)\left(\frac{b_1 I(t)}{N} + b_0 - c\right) < \infty.$$

Now here, first note that only value in the denominator N_h, which by our initial conditions will always be non zero (The total human population will never be zero.) Thus, for any values of f_i, we will not have a partial derivative that diverges to ∞. Additionally, We note that the operations involved are addition, subtraction, multiplication and division, thus, we can claim easily that all the $\frac{\partial f_i}{\partial x_j}$ are continuous as well. □

3.2. Invariance of the Solution

The feasible solution set which is positively invariant $\mho = \{(S, V, E, L_f, L_s, I, D, R, x) \in \mathbb{R}_+^9 : N \leq \frac{\Lambda}{\mu}$ and $x \leq 1\}$ with $N = S + V + E + L_f + L_s + I + D + R$

Theorem 3.3. *The set $\mho$ is positively invariant and attracts all solutions in $\mathbb{R}_+^{12}$*

Proof. Consider $N = S + V + E + L_f + L_s + I + D + R$. Add the equations (2.1) to (3.12) to obtain

$$\begin{aligned}
\frac{dN}{dt} &= \frac{dS}{dt} + \frac{dV}{dt} + \frac{dE}{dt} + + \frac{dL_f}{dt} + \frac{dL_s}{dt} + \frac{dI}{dt} + \frac{dD}{dt} + \frac{dR}{dt} \\
\frac{dN_h}{dt} &= \Lambda - \mu(S + V + E + L_f + L_s + I + D + R) - \mu_T I - (1-\sigma)\tau D \\
\frac{dN_h}{dt} &\leq \Lambda - \mu(S + V + E + L_f + L_s + I + D + R) \\
\frac{dN_h}{dt} &\leq \Lambda - \mu N
\end{aligned}$$

From the above, we can obtain a first order linear differential equation of the form

$$\frac{dN_h}{dt} + \mu N = \Lambda.$$

Take the Integrating Factor as $e^{\int \mu dt}$ and solving, we obtain the solution

$$N \leq N_0 e^{-\mu t} + \frac{\Lambda}{\mu}(1 - e^{-\mu t})$$

Take $\lim_{t\to\infty}$ and we get

$$N_h \leq \frac{\Lambda}{\mu}.$$

Finally, consider the IKS dynamics.

$$\begin{aligned}
\frac{dx}{dt} &= vx(1-x)(b_0 + b_1\left(\frac{I}{N}\right) - C) \\
\frac{dx}{dt} &\leq vx(1-x)(b_0 + b_1 - C) \text{ as } \frac{I_s}{N_h} \leq 1
\end{aligned}$$

Suppose $\frac{d\hat{x}}{dt} = vx(1-x)(b_0 + b_1 - C)$. Again this is a simple first order differential equation. We solve it to find

$$\hat{x} = \frac{x_0 e^{v(b_0+b_1-C)t}}{1 - x_0 + x_0 e^{v(b_0+b_1-C)t}}.$$

Take $\lim_{t\to\infty}$ we get

$$\hat{x} \leq 1$$

By comparision principle,

$$x \leq 1$$

. Hence the set $\mho$ is positively invariant and attracts all solutions in $\mathbb{R}^9_+$ □

3.3. Positivity and boundedness of the model

Theorem 3.4. *The set* $\{\mho = (S(0), V(0), E(0), L_f(0), L_s(0), I(0), D(0), R(0), x(0)) \in \mathbb{R}^9_+\}$ *is the closed region for our model with non negative initial conditions for all solutions initiating in the positive orthant.*

Proof. We want to check that each hyperplane bounds the positive orthant in vector field $\mathbb{R}^9_+$ to show

the positivity of solutions.

$$\begin{aligned}
\dot{S}(t)\Big|_{S=0} &= \Lambda - \lambda S - \phi(x) + \omega_V V - \mu_h S \\
&= \Lambda + \omega_V V \geq 0 \\
\dot{V}(t)\Big|_{V=0} &= \phi(x)S - \lambda_V V - \omega_V V - \mu V \\
&= \phi(x)S \geq 0 \\
\dot{E}(t)\Big|_{E=0} &= \lambda S + \lambda_V V + \lambda_R - (\gamma + \mu)E \\
&= \lambda S + \lambda_V V + \lambda_R \geq 0 \\
\dot{L_f}(t)\Big|_{L_f=0} &= p\gamma E - (\kappa_f + \mu)L_f \\
&= p\gamma E \geq 0 \\
\dot{L_s}(t)\Big|_{L_s=0} &= (1-p)\gamma E - (\kappa_s + \mu)L_s \\
&= (1-p)\gamma E \geq 0 \\
\dot{I}(t)\Big|_{I=0} &= \kappa_f L_f + \kappa_s L_s - (\delta + \mu + \mu_T)I \\
&= \kappa_f L_f + \kappa_s L_s \geq 0 \\
\dot{D}(t)\Big|_{D=0} &= \delta I - (\tau + \mu)D \\
&= \delta I \geq 0 \\
\dot{R}(t)\Big|_{R=0} &= \sigma\tau D - (\alpha_R + \lambda_R + \mu)R \\
&= \sigma\tau D \geq 0 \\
\dot{x}(t)|_{x=0} &= vx(1-x)(B(x) - C) \\
&= 0 \geq 0
\end{aligned}$$

Thus, the solution from the above set will continue to lie in $\mathbb{R}^{12}_+$, that gives us the bounded feasible region as follows
$\mho = \{(S(0), V(0), E(0), L_f(0), L_s(0), I(0), D(0), R(0), x(0)) \in \mathbb{R}^9_+\}$ □

4. Basic Reproduction Number R_0

We can calculate the equilibrium points by putting (2.1) as 0. We get the Disease Free Equilibrium E^0 as :

$$E^0 = \left\{ \frac{\Lambda(\mu + \omega_V)}{\mu(\mu + \omega_V + \phi)}, \frac{\Lambda(\phi)}{\mu(\mu + \omega_V + \phi)}, 0, 0, 0, 0, 0, 0, x \right\}$$

where x = 0 or 1. We use the Next Generation Matrix Method to find R_0. We have the required infectious subsystem :

$$\begin{aligned}
\dot{E}(t) &= \lambda S + \lambda_V V + \lambda_R - (\gamma + \mu)E \\
\dot{L_f}(t) &= p\gamma E - (\kappa_f + \mu)L_f \\
\dot{L_s}(t) &= (1-p)\gamma E - (\kappa_s + \mu)L_s \\
\dot{I}(t) &= \kappa_f L_f + \kappa_s L_s - (\delta + \mu + \mu_T)I \\
\dot{D}(t) &= \delta I - (\tau + \mu)D
\end{aligned}$$

From the RHS of the above infectious subsystem , we construct $\mathscr{F}$ and $\mathscr{V}$ which represent the rates of new infection and the transition between compartments for the entire system.

$$\text{Consider F} = \begin{pmatrix} \frac{\beta\rho_R R(t)(\eta_D D+I)}{N} + \frac{\beta S(t)(\eta_D D+I)}{N} + \frac{\beta(1-\varepsilon_S)V(t)(\eta_D D+I)}{N} \\ 0 \\ 0 \\ 0 \\ 0 \end{pmatrix}$$

$$\text{and V} = \begin{pmatrix} (\gamma+\mu)E \\ (\kappa_f+\mu)L_f - \gamma pE \\ L_s(\mu+\kappa_s) - \gamma(1-p)E \\ I(\delta+\mu+\mu_T) - \kappa_s L_s - \kappa_f L_f \\ (D(\mu+\tau)) - \delta I \end{pmatrix}$$

Let $\mathscr{F}$ and $\mathscr{V}$ be $\left(\frac{\partial F_i}{\partial x_j}\right)$ and $\left(\frac{\partial V_i}{\partial x_j}\right)$ where $x_j \in \{E, I_a, I_s, H, E_v, I_v\}$ respectively. Thus we get

$$\mathscr{F} = \begin{pmatrix} 0 & 0 & 0 & \frac{\beta\Lambda(\mu-\phi\varepsilon_S+\omega_V+\phi)}{\mu\text{Nh}(\mu+\omega_V+\phi)} & \frac{\beta\Lambda\eta_{\text{Di}}(\mu-\phi\varepsilon_S+\omega_V+\phi)}{\mu\text{Nh}(\mu+\omega_V+\phi)} \\ 0 & 0 & 0 & 0 & 0 \\ 0 & 0 & 0 & 0 & 0 \\ 0 & 0 & 0 & 0 & 0 \\ 0 & 0 & 0 & 0 & 0 \end{pmatrix}$$

$$\text{and } \mathscr{V} = \begin{pmatrix} \gamma+\mu & 0 & 0 & 0 & 0 \\ \gamma(-p) & \kappa_f+\mu & 0 & 0 & 0 \\ \gamma(p-1) & 0 & \mu+\kappa_s & 0 & 0 \\ 0 & -\kappa_f & -\kappa_s & \delta+\mu+\mu_T & 0 \\ 0 & 0 & 0 & -\delta & \mu+\tau \end{pmatrix}$$

$$\mathscr{V}^{-1} = \begin{pmatrix} \frac{1}{\gamma+\mu} & 0 & 0 & 0 & 0 \\ \frac{\gamma p}{(\gamma+\mu)(\kappa_f+\mu)} & \frac{1}{\kappa_f+\mu} & 0 & 0 & 0 \\ \frac{\gamma(p+1)}{(\gamma+\mu)(\mu+\kappa_s)} & 0 & \frac{1}{\mu+\kappa_s} & 0 & 0 \\ \frac{\gamma(\kappa_f(\mu p+\kappa_s)+\mu(1-p)\kappa_s)}{(\gamma+\mu)(\kappa_f+\mu)(\mu+\kappa_s)(\delta+\mu+\mu_T)} & \frac{\kappa_f}{(\kappa_f+\mu)(\delta+\mu+\mu_T)} & \frac{\kappa_s}{(\mu+\kappa_s)(\delta+\mu+\mu_T)} & \frac{1}{\delta+\mu+\mu_T} & 0 \\ \frac{\gamma\delta(\kappa_f(\mu p+\kappa_s)+\mu(1-p)\kappa_s)}{(\gamma+\mu)(\mu+\tau)(\kappa_f+\mu)(\mu+\kappa_s)(\delta+\mu+\mu_T)} & \frac{\delta\kappa_f}{(\mu+\tau)(\kappa_f+\mu)(\delta+\mu+\mu_T)} & \frac{\delta\kappa_s}{(\mu+\tau)(\mu+\kappa_s)(\delta+\mu+\mu_T)} & \frac{\delta}{(\mu+\tau)(\delta+\mu+\mu_T)} & \frac{1}{\mu+\tau} \end{pmatrix}$$

The required R_0 is given by the formula $\rho(-\mathscr{F}\mathscr{V}^{-1})$ where ρ is the linear span (maximum magnitude of the eigenvalue). Thus, we obtain the value of R_0 as :

$$R_0 = \frac{\beta\gamma(\delta\eta_D+\mu+\tau)(\kappa_f(\mu p+\kappa_s)+\mu(1-p)\kappa_s)(\mu+\phi(1-\varepsilon_S)+\omega_V)}{(\gamma+\mu)(\mu+\tau)(\kappa_f+\mu)(\mu+\kappa_s)(\delta+\mu+\mu_T)(\mu+\omega_V+\phi)}$$

5. Stability Analysis

Stability analysis forms the mathematical cornerstone for understanding whether an infectious disease will persist or be eliminated from a population. This section investigates the stability properties of the TB-IKS model's equilibria, with particular attention to how IKS adoption dynamics modify conventional stability thresholds. We begin by analyzing the disease-free equilibrium (DFE), determining conditions under which TB naturally dies out. We then examine the endemic equilibrium, identifying parameter regimes where the disease persists at a steady state. The analysis employs a combination of linear stability methods, Lyapunov theory, and center manifold techniques to provide both local and global perspectives on system behavior. Importantly, we explore how the incorporation of IKS practices alters the bifurcation structure of the model, revealing nuanced relationships between behavioral adaptation and epidemiological outcomes.

5.1. Local Stability of Disease Free equilibrium point

Theorem 5.1. *The disease free equilibrium E^0 is locally asymptotically stable when $R_0 < 1$ and unstable when $R_0 > 1$.*

Proof. Consider the Jacobian of the system of (2.1) to (3.12) at E^0. The characteristic equation we get is
$$\frac{\beta\delta l_4 l_8 \eta_D(\mu+q)\,(b_0 v - cv - q)\,(-\mu - q - \alpha_R)\,(\mu + q + \omega_V + \phi)}{\mu + \omega_V + \phi}$$
$$-\,(l_5+q)\,(\beta\gamma l_4\,((p-1)\,(l_6+q)\,\kappa_s - p\kappa_f\,(l_2+q)) + l_3\,(l_1+q)\,(l_2+q)\,(l_6+q)\,(l_7+q)).$$
On expanding the last factor, we get $e_0 = l_3$
$e_1 = l_1l_3 + l_2l_3 + l_5l_3 + l_6l_3 + l_7l_3$
$e_2 = l_1l_2l_3 + l_1l_5l_3 + l_2l_5l_3 + l_1l_6l_3 + l_2l_6l_3 + l_5l_6l_3 + l_1l_7l_3 + l_2l_7l_3 + l_5l_7l_3 + l_6l_7l_3$
$e_3 = l_1l_2l_3l_5 + l_1l_3l_6l_5 + l_2l_3l_6l_5 + l_1l_3l_7l_5 + l_2l_3l_7l_5 + l_3l_6l_7l_5 + l_1l_2l_3l_6 + l_1l_2l_3l_7 + l_1l_3l_6l_7 + l_2l_3l_6l_7 - p\beta\gamma l_4\kappa_f + p\beta\gamma l_4\kappa_s - \beta\gamma l_4\kappa_s$
$e_4 = l_1l_2l_3l_4l_6 + l_1l_2l_3l_7l_6 + l_1l_3l_4l_7l_6 + l_2l_3l_4l_7l_6 + l_1l_2l_3l_8l_6 + l_1l_3l_4l_8l_6 + l_2l_3l_4l_8l_6 + l_1l_3l_7l_8l_6 + l_2l_3l_7l_8l_6 + l_3l_4l_7l_8l_6 + l_1l_2l_3l_4l_7 + l_1l_2l_3l_4l_8 + l_1l_2l_3l_7l_8 + l_1l_3l_4l_7l_8 + l_2l_3l_4l_7l_8 - (\delta\sigma\tau l_3\alpha_R + p\beta\gamma l_5\,(l_2 + l_4 + l_6 + \delta\eta_D))\,\kappa_f + (p-1)\beta\gamma l_5\,(l_4 + l_6 + l_7 + \delta\eta_D)\,\kappa_s$
$e_5 = l_1l_2l_3l_5l_6 + l_1l_2l_3l_7l_6 + l_1l_3l_5l_7l_6 + l_2l_3l_5l_7l_6 + p\beta\gamma l_4\kappa_s l_6 - \beta\gamma l_4\kappa_s l_6 + l_1l_2l_3l_5l_7 - p\beta\gamma l_2l_4\kappa_f - p\beta\gamma l_4l_5\kappa_f + p\beta\gamma l_4l_5\kappa_s - \beta\gamma l_4l_5\kappa_s$
$e_6 = l_1l_2l_3l_5l_6l_7 + \beta\delta l_4l_8\eta_D - p\beta\gamma l_2l_4l_5\kappa_f + p\beta\gamma l_4l_5l_6\kappa_s - \beta\gamma l_4l_5l_6\kappa_s.$
We need to prove that the coefficients of the characteristic polynomial satisfy the Routh - Hurwitz Criterion to establish stability at $R_0 < 1$. The necessary condition is that e_1, e_2, e_3, e_4, e_5 are all positive. We can observe that e_0, e_1, e_2 are always positive. Also, e_3, e_4, e_5, e_6 are all positive when $R_0 < 1$
Now we show that all the Hurwitz Determinants are positive. First we find the Hurwitz matrix H :

$$H = \begin{pmatrix} e_1 & e_3 & e_5 & 0 & 0 & 0 \\ e_0 & e_2 & e_4 & e_6 & 0 & 0 \\ 0 & e_1 & e_3 & e_5 & 0 & 0 \\ 0 & e_0 & e_2 & e_4 & e_6 & 0 \\ 0 & 0 & e_1 & e_3 & e_5 & 0 \\ 0 & 0 & e_0 & e_2 & e_4 & e_6 \end{pmatrix}$$

The Hurwitz Determinants, represented by Δ_i where $i = 1, 2, 3, 4, 5$:

$$\begin{aligned}
\Delta_1 &= e_1 \\
\Delta_2 &= e_1e_2 - e_0e_3 \\
\Delta_3 &= e_3\Delta_2 - e_1^2e_4 + e_0e_1e_5 \\
\Delta_4 &= e_4\Delta_3 + e_2e_6e_1^2 + e_0e_4e_5e_1 - e_0e_3e_6e_1 - e_0^2e_5^2 - e_1e_2^2e_5 + e_0e_2e_3e_5 \\
\Delta_5 &= e_5\Delta_4 - e_6^2e_1^3 + e_3e_4e_6e_1^2 + e_2e_5e_6e_1^2 - e_2e_3^2e_6e_1 - 2e_0e_3e_5e_6e_1 + e_0e_3^3e_6 \\
\Delta_6 &= e_6\Delta_5
\end{aligned}$$

We can see that all Hurwitz determinants are positive when $R_0 < 1$. Thus, E^0 is the asymptotically stable locally when $R_0 < 1$. Note that if $R_0 > 1$, $e_3, e_4, e_5, e_6 \leq 0$ and thus the necessary condition for stability fails. □

5.2. Global Stability of Disease Free equilibrium point

Theorem 5.2. *The disease free equilibrium E^0 is globally asymptotically stable when $R_0 < 1$*

Proof. Consider the following linear Lyapunov function candidate :
$L(X(t)) = a_1E + a_2L_f + a_3L_s + a_4L_f + a_5I$ where
$$a_1 = \frac{\gamma\,(\kappa_f\,(\mu p + \kappa_s) - \mu(p-1)\kappa_s)}{(\gamma+\mu)\,(\kappa_f+\mu)}$$

$$a_2 = \frac{\kappa_f\left(\mu+\kappa_s\right)}{\kappa_f+\mu}$$
$$a_3 = \kappa_s$$
$$a_4 = \mu+\kappa_s$$
$$a_5 = \frac{\beta\gamma\eta_D\left(-\varepsilon_S V^0+S^0+V^0\right)\left(\kappa_f\left(\mu p+\kappa_s\right)+\mu(1-p)\kappa_s\right)}{N(\gamma+\mu)(\mu+\tau)\left(\kappa_f+\mu\right)}$$

We take the derivative of L w.r.t to t.

$$\begin{aligned}\dot{L}(X(t)) &= a_1\dot{E}+a_2\dot{L}_f+a_3\dot{L}_s+a_4\dot{L}_f+a_5\dot{I}\\ &= I(t)\frac{\left(\delta\eta_D+\mu+\tau\right)\left(\beta\gamma\left(S(t)(1-\varepsilon_S)V(t)\right)\left(\kappa_f\left(\mu p+\kappa_s\right)+\mu(1-p)\kappa_s\right)\right)}{N(\gamma+\mu)(\mu+\tau)\left(\kappa_f+\mu\right)}\\ &\quad-\frac{N(\gamma+\mu)(\mu+\tau)\left(\kappa_f+\mu\right)\left(\mu+\kappa_s\right)\left(\delta+\mu+\mu_T\right)}{N(\gamma+\mu)(\mu+\tau)\left(\kappa_f+\mu\right)}\\ &\leq (R_0-1)(\mu+\kappa_s)(\delta+\mu+\mu_T)I\end{aligned}$$

When $R_0 < 1$, then $\dot{L}(t) \leq 0$. $Clearly L(X(t)) \geq 0$ for all $X(t) \in \mathbb{R}^9_+$. $L(X(t)) = 0$ when $I = 0$ or at $R_0 = 1$ which implies that $L(X(t)) = 0$ when $X(t) = E^0$. So $L(X(t))$ is a Lyapunov function on $\mathbb{R}^9_+$ and E^0 is the largest compact invariant set such that $L(X(t)) = 0$, so by LaSalle's Invariance Principle, E^0 is globally asymptotically stable. □

5.3. Existence of Endemic Equilibrium Point

In this section we find the condition for existence of endemic equilibrium point for the model. Let $E^*_q = \{S^*, V^*, E^*, L^*_f, L^*_s, I^*, D^*, R^*, x^*\}$ be the endemic equilibrium obtained from the steady state of the model. The components of E^* are :

$$\begin{aligned}S^* &= \frac{\Lambda\left(\mu+\lambda_V+\omega_V\right)}{(\lambda+\mu)\omega_V+\left(\lambda+\mu+\phi\right)\left(\mu+\lambda_V\right)}\\ V^* &= \frac{\Lambda\phi}{(\lambda+\mu)\omega_V+\left(\lambda+\mu+\phi\right)\left(\mu+\lambda_V\right)}\\ E^* &= \frac{\lambda S^*+\lambda_V V^*+\lambda_R R^*}{\gamma+\mu}\\ L^*_f &= \frac{\gamma p\mathrm{Es}(t)}{\kappa_f+\mu}\\ L^*_s &= \frac{\gamma(1-p)\mathrm{Es}(t)}{\mu+\kappa_s}\\ I^* &= \frac{(\mu+\tau)\left(\kappa_f L^*_f+\kappa_s L^*_s\right)}{(\delta+\mu+\mu_T)}\\ D^* &= \frac{\delta I}{\mu+\tau}\\ R^* &= \frac{\delta\sigma\tau I^*}{\left(\mu+\tau\right)\left(b\ I^*\rho_R+\mu+\alpha_R\right)}\\ x^* &= 0 \text{ or } 1\end{aligned}$$

where $b = \frac{\beta\left(\delta\eta_D+\mu+\tau\right)}{N(\mu+\tau)}$

Now we substitute the values of L^*_f and L^*_s into the equation for I^* and then solve for I^*. We get

$c_0(I^*)^3 + c_1(I^*)^2 + c_2 I^* + c_3 = 0$, where

$$
\begin{aligned}
c_0 &= b^3\gamma\delta\sigma\tau(\kappa_f(\mu p+\kappa_s)+\mu(1-p)\kappa_s)(\rho_R(1-\varepsilon_S)+\Lambda(\mu+\tau)(\mu+\alpha_R)(\mu-\phi\varepsilon_S+\omega_V+\phi))\\
&\quad+(\gamma+\mu)(\mu+\tau)(\kappa_f+\mu)(\mu+\kappa_s)(\delta+\mu+\mu_T)(b^3\rho_R(1-\varepsilon_S)+\mu\omega_V(\mu+\alpha_R)),\\
c_1 &= \mu(\gamma+\mu)(\mu+\tau)(\mu+\phi)(\kappa_f+\mu)(\mu+\alpha_R)(\mu+\kappa_s)(\delta+\mu+\mu_T),\\
c_2 &= b(b(\gamma+\mu)(\mu+\tau)(\kappa_f+\mu)(\mu+\kappa_s)(\delta+\mu+\mu_T)((1-\varepsilon_s)(\mu+\alpha_R+\mu\rho_R+\phi\rho_R)+\rho_R(\mu+\omega_v))\\
&\quad-b\gamma\rho_R(\kappa_f(\mu p+\kappa_s)+\mu(1-p)\kappa_s)((1-\varepsilon_s)(b\Lambda(\mu+\tau)+\delta\sigma\tau(\mu+\phi))+\delta\sigma\tau(\mu+\omega_V)))\\
c_3 &= b(\gamma+\mu)(\mu+\tau)(\kappa_f+\mu)(\mu+\kappa_s)(\delta+\mu+\mu_T)((\mu+\phi)(1-\varepsilon_s)(\mu+\alpha_R)+(\mu+\alpha_R)(\mu+\omega_V)\\
&\quad+\mu\rho_R(\mu+\omega_V+\phi))-b\gamma(\kappa_f(\mu p+\kappa_s)+\mu(1-p)\kappa_s)(b\Lambda(\mu+\tau)((1-\varepsilon_s)(\mu+\alpha_R+\phi\rho_R)\\
&\quad+\rho_R(\mu+\omega_V))+\delta\mu\sigma\tau\rho_R(\mu+\omega_V+\phi))
\end{aligned}
$$

Here, note that $c_0, c_1 > 0$ always, and when $R_0 > 1$, then $c_2, c_3 < 0$. This means there is one sign change in the equation for I^*. By Descartes Rule of Sign, this implies there will be one positive real value of I^* when $R_0 > 1$. When $R_0 < 1$, then there will be no sign change so there will be no positive root. Thus the endemic equilibrium E_q^* exists when $R_0 > 1$.

5.4. Local Stability of Endemic Equilibrium

Theorem 5.3. *The Endemic Equilibrium E_q^* is locally asymptotically stable when $R_0 > 1$.*

Proof. To prove this result, we employ center manifold theory. First, we write the variables as $x = (x_1, x_2, x_3, x_4, x_5, x_6, x_7, x_8, x_9)^T$ where $S = x_1$, $V = x_2$, $E = x_3$, $L_f = x_4$, $L_s = x_5$, $I = x_6$, $D = x_7$, $R = x_8$, $x = x_9$, and $\frac{dx}{dt} = \{f_i(x, \beta), i = 1, 2, \ldots, 9\}$. The model in terms of new variables is:

$$
\begin{aligned}
\dot{x}_1 &= \Lambda + x_2\omega_V - \lambda x_1 - \mu x_1 - \phi x_1\\
\dot{x}_2 &= -x_2\lambda_V - x_2\omega_V - \mu x_2 + \phi x_1\\
\dot{x}_3 &= \lambda_R x_8 + x_2\lambda_V - (\gamma+\mu)x_3 + \lambda x_1\\
\dot{x}_4 &= \gamma p x_3 - x_4(\kappa_f+\mu)\\
\dot{x}_5 &= \gamma(1-p)x_3 - x_5(\mu+\kappa_s)\\
\dot{x}_6 &= \kappa_f x_4 + \kappa_s x_5 - x_6(\delta+\mu+\mu_T)\\
\dot{x}_7 &= \delta x_6 - (\mu+\tau)x_7\\
\dot{x}_8 &= \sigma\tau x_7 - x_8(\mu+\alpha_R+\lambda_R)\\
\dot{x}_9 &= x_9(1-x_9)v(B-c)
\end{aligned}
$$

We choose β as the bifurcation parameter. At $R_0 = 1$,

$$
\beta = \beta^* = \frac{(\gamma+\mu)(\mu+\tau)(\kappa_f+\mu)(\mu+\kappa_s)(\delta+\mu+\mu_T)(\mu+\omega_V+\phi)}{\gamma(\delta\eta_D+\mu+\tau)(\kappa_f(\mu p+\kappa_s)+\mu(1-p)\kappa_s)(\mu+\phi(1-\varepsilon_S)+\omega_V)}.
$$

We find $A = D_x f(0, 0)$:

$$
A = \begin{pmatrix}
-\mu-\phi & \omega_V & 0 & 0 & 0 & 0 & 0 & 0 & 0\\
\phi & -\mu-\omega_V & 0 & 0 & 0 & 0 & 0 & 0 & 0\\
0 & 0 & -\gamma-\mu & 0 & 0 & 0 & 0 & 0 & 0\\
0 & 0 & \gamma p & -\kappa_f-\mu & 0 & 0 & 0 & 0 & 0\\
0 & 0 & \gamma(1-p) & 0 & -\mu-\kappa_s & 0 & 0 & 0 & 0\\
0 & 0 & 0 & \kappa_f & \kappa_s & -\delta-\mu-\mu_T & 0 & 0 & 0\\
0 & 0 & 0 & 0 & 0 & \delta & -\mu-\tau & 0 & 0\\
0 & 0 & 0 & 0 & 0 & 0 & \sigma\tau & -\mu-\alpha_R & 0\\
0 & 0 & 0 & 0 & 0 & 0 & 0 & 0 & -v(b_0-c)
\end{pmatrix}.
$$

Note that when $\beta^* = 0$, at least one factor in the numerator vanishes, causing one diagonal element to be zero, giving one simple eigenvalue of 0 while all others are negative. This allows us to use Theorem 4.1 from [6].

The right eigenvector $w = (w_1, w_2, w_3, w_4, w_5, w_6, w_7, w_8, w_9)^T$ is:

$$\begin{aligned}
w_1 &= w_2 = 0,\\
w_3 &= w_3 > 0,\\
w_4 &= \frac{\gamma p w_3}{\kappa_f + \mu},\\
w_5 &= \frac{\gamma(1-p)w_3}{\mu + \kappa_s},\\
w_6 &= \frac{\gamma w_3(\kappa_f(\mu p + \kappa_s) + \mu(1-p)\kappa_s)}{(\kappa_f + \mu)(\mu + \kappa_s)(\delta + \mu + \mu_T)},\\
w_7 &= \frac{\delta\gamma w_3(\kappa_f(\mu p + \kappa_s) + \mu(1-p)\kappa_s)}{(\mu + \tau)(\kappa_f + \mu)(\mu + \kappa_s)(\delta + \mu + \mu_T)},\\
w_8 &= \frac{\delta\gamma\sigma\tau w_3(\kappa_f(\mu p + \kappa_s) + \mu(1-p)\kappa_s)}{(\mu + \tau)(\kappa_f + \mu)(\mu + \alpha_R)(\mu + \kappa_s)(\delta + \mu + \mu_T)},\\
w_9 &= 0.
\end{aligned}$$

The left eigenvector $v = (v_1, v_2, v_3, v_4, v_5, v_6, v_7, v_8, v_9)$ is:

$$\begin{aligned}
v_1 &= v_2 = 0,\\
v_3 &= \frac{\gamma v_5(\kappa_f(\mu p + \kappa_s) - \mu(p-1)\kappa_s)}{(\gamma + \mu)\kappa_s(\kappa_f + \mu)},\\
v_4 &= \frac{v_5\kappa_f(\mu + \kappa_s)}{\kappa_s(\kappa_f + \mu)},\\
v_5 &= v_5 > 0,\\
v_6 &= \frac{v_5(\mu + \kappa_s)}{\kappa_s},\\
v_7 &= \frac{v_5(\mu + \kappa_s)(\delta + \mu + \mu_T)}{\delta\kappa_s},\\
v_8 &= v_9 = 0.
\end{aligned}$$

We now compute

$$a = \sum_{k,i,j=1}^{9} v_k w_i w_j \frac{\partial^2 f_k(0,0)}{\partial x_i \partial x_j} \quad \text{and} \quad b = \sum_{k,i=1}^{9} v_k w_i \frac{\partial^2 f_k(0,0)}{\partial x_i \partial \beta}.$$

After calculation:

$$a = \frac{2\beta\gamma^2\delta\sigma\tau v_5 w_3^2 \rho_R(\delta\eta_D + \mu + \tau)(\kappa_f(\mu p + \kappa_s) + \mu(1-p)\kappa_s)^3}{N(\gamma + \mu)^2(\mu + \tau)^2\kappa_s(\kappa_f + \mu)^3(\mu + \alpha_R)(\mu + \kappa_s)^2(\delta + \mu + \mu_T)^2} > 0,$$

and

$$\begin{aligned}
b =& \frac{\gamma v_5 w_3(\kappa_f(\mu p + \kappa_s) + \mu(1-p)\kappa_s)^2}{N(\gamma + \mu)(\mu + \tau)\kappa_s(\kappa_f + \mu)^2(\mu + \alpha_R)(\mu + \kappa_s)(\delta + \mu + \mu_T)}\\
&\times \Big[(\mu + \alpha_R)(\delta\eta_D + \mu + \tau)((1 - \varepsilon_S)x_2 + \rho_R x_8 + x_1)\\
&+ \rho_R\delta\sigma\tau(\eta_D x_7 + x_6)\Big] > 0.
\end{aligned}$$

Both a and b are positive. By case (i) of Theorem 4.1 in [6], E_q^* is locally asymptotically stable. By Corollary 4.1, the bifurcation at β^* is backward. □

5.5. Global Stability of Endemic Equilibrium

Lemma 5.1. *Consider the following function defined as*

$$g(x) = x - x^* - x^* \ln\left(\frac{x}{x^*}\right), \ x, x^* \in \mathbb{R}^+.$$

Then $g(x) \geq 0 \ \forall x, x^* \in \mathbb{R}^+$.

Proof. Consider first and second derivatives $g'(x) = 1 - \frac{x^*}{x}, g''(x) = \frac{x^*}{x^2}$. The critical point is then $x = x^*$ and since $g''(x^*) = \frac{1}{x^*} > 0$ when $x^* > 0$. We have global minima at $x = x^*$ which is $g(x^*) = 0$. Thus $g(x) \geq 0 \ \forall x, x^* \in \mathbb{R}^+$ □

Theorem 5.4. *The Endemic Equilibrium* E_q^* *is globally asymptotically stable when* $R_0 > 1$.

Proof. Consider the Liapunov function candidate :
$V(X(t)) = (S - S^*) + (V - V^*) + (E - E^*) + (L_f - L_f^*) + (L_s - L_s^*) + (I - I^*) + (D - D^*) + (R - R^*)$
$- (S^* + V^* + E^* + L_f^* + L_s^* + I^* + D^* + R^*) \ln\left(\frac{S + V + E + L_f + L_s + I + D + R}{S^* + V^* + E^* + L_f^* + L_s^* + I^* + D^* + R^*}\right)$
$+ (x - x^*) - x^* \ln\left(\frac{x}{x^*}\right).$
Clearly $V(E_q^*) = 0$.
Also, we can write $V(X(t))$ as
$V(X(t)) = N - N^* - N^* \ln\left(\frac{N}{N^*}\right)$
$+ x - x^* - x^* \ln\left(\frac{x}{x^*}\right).$
From Lemma (5.1), we get $V(X(t)) > 0 \ \forall X(t) \neq E^*$.
Now, consider the derivative with respect to time.

$$\begin{aligned}
\dot{V}(X(t)) &= \left(1 - \frac{N^*}{N}\right)\dot{N} + \left(1 - \frac{x^*}{x}\right)\dot{x} \\
&\leq \left(1 - \frac{N^*}{N}\right)(\Lambda_h - \mu_h N) + \left(1 - \frac{1}{x}\right)(vx(1-x)(b_0 + b_1 - C)) \\
&= \left(1 - \frac{N^*}{N}\right)(\mu N^* - \mu N) + \left(\frac{x-1}{x}\right)(vx(1-x)(b_0 + b_1 - C)) \\
&= -\mu\left(\frac{(N - N^*)^2}{N}\right) - v(1-x)^2(b_0 + b_1 - C) \\
&\leq 0
\end{aligned}$$

Since $X(t) = E_q^*$ is the only point where $\dot{V}(X(t)) = 0$, then by LaSalle's Invariance Principle, E_q^* is globally asymptotically stable. □

6. Sensitivity Analysis

To identify key parameters driving tuberculosis transmission within our model, we perform a sensitivity analysis of the basic reproduction number R_0. Specifically, we compute the Normalized Forward Sensitivity Index (NFSI) for each parameter m that appears in R_0, defined as:

$$\psi_m^{R_0} = \frac{\partial R_0}{\partial m} \cdot \frac{m}{R_0}. \tag{6.1}$$

This index quantifies the proportional change in R_0 resulting from a small proportional change in m. For instance, the transmission rate β has an NFSI of $+1$, indicating that a 1% increase in β yields a 1% increase in R_0.

Using the baseline parameter values from Table **??**, which yield $R_0 = 2.60483$, we compute sensitivity indices for all relevant parameters. Results are summarized in the bar chart in Figure X, where positive values denote parameters that amplify transmission when increased, and negative values denote parameters that suppress transmission when increased.

6.1. Interpretation of Sensitivity Indices

The analysis reveals several critical insights:

- The transmission coefficient β exhibits the highest positive sensitivity ($\psi_\beta^{R_0} = +1$), confirming its role as the primary driver of TB spread.

- Following β, the relative infectiousness of diagnosed individuals (η_D) shows substantial positive sensitivity, highlighting the importance of early case detection and isolation in reducing transmission.

- Among parameters with negative sensitivity, the IKS efficacy parameter ε_S stands out with the strongest inhibitory effect ($\psi_{\varepsilon_S}^{R_0} < 0$). This indicates that even moderate levels of IKS effectiveness (here assumed to be 60%) can substantially lower R_0, underscoring the potential of culturally-grounded behavioral interventions.

- Other parameters with notable negative indices include natural mortality (μ), TB-induced mortality (μ_T), treatment initiation (τ), and detection rate (δ). This suggests that coupling IKS adoption with enhanced diagnosis and treatment can synergistically suppress transmission.

- IKS adoption parameters (μ_a, κ_a) exhibit modest negative sensitivity in the baseline scenario, reflecting their indirect influence via ε_S. Their impact grows under higher adoption rates or when integrated with community-based promotion strategies.

6.2. Contour Analysis of Key Parameters

To further elucidate how sensitive parameters interact with β to shape R_0, we generate contour plots of R_0 as a function of β paired with each negatively sensitive parameter. As seen in Figure 3a, parameters with strong negative sensitivity (e.g., ε_S) produce steep gradients, meaning that modest improvements in IKS efficacy can offset substantial increases in transmission risk. In contrast, parameters with weaker sensitivity (e.g., κ_a) yield flatter contours (Figure 3g), indicating that their influence on R_0 is comparatively modest unless coupled with complementary interventions.

These findings collectively emphasize that TB control in India could benefit from integrated strategies that combine conventional biomedical measures (enhancing δ, τ, and reducing η_D) with culturally-informed behavioral programs that leverage IKS practices to increase ε_S and adoption rates. It is important to note that the sensitivity indices reported here are derived under the assumption of uniform parameter values across the population. In a geographically heterogeneous setting, the relative importance of parameters may shift. For example, in high-burden states with intense transmission, parameters such as β and η_D are likely to dominate the dynamics, whereas in regions with stronger cultural adherence to traditional practices, IKS-related parameters like ε_S and μ_a could play a more decisive role in modulating R_0. This suggests that sensitivity-guided interventions should be spatially tailored, combining biomedical measures in high-transmission zones with culturally informed behavioural programmes in areas where IKS adoption is more readily accepted.

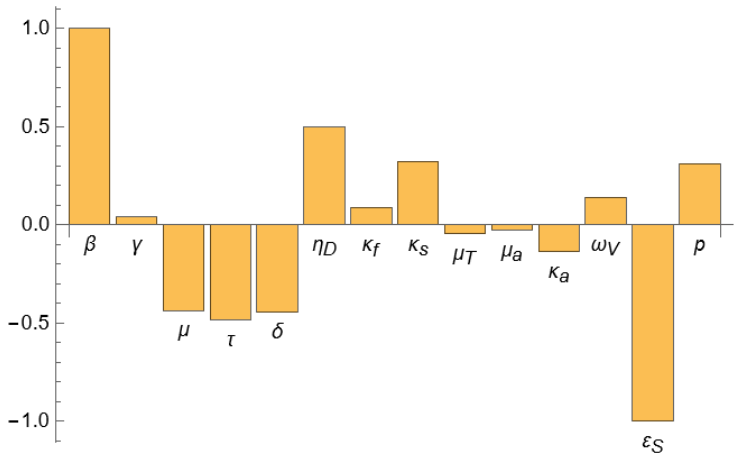

Figure 2: Normalised Forward Sensitivity Index of R_0

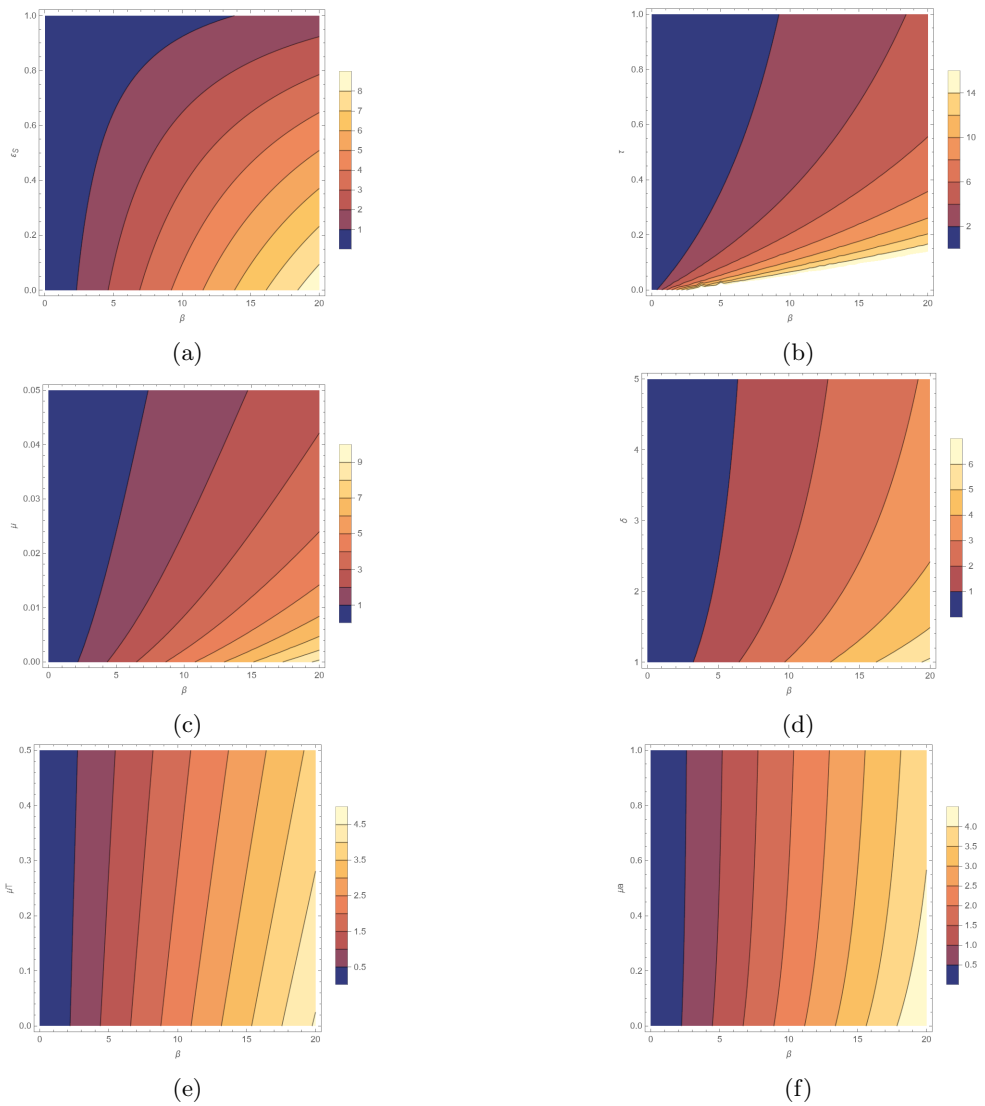

(a) (b) (c) (d) (e) (f)

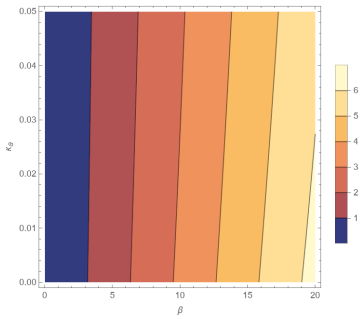

(g)

Figure 3: Contour plot of R_0 as a function of transmission rate β and parameters ε_S, τ, μ, δ, μ_T, μ_a, κ_a respectively

7. Numerical Simulation and Validation

This section presents numerical simulations of the proposed TB-IKS model to validate the analytical results derived in previous sections and to illustrate the epidemiological implications of the model dynamics. All simulations employ the baseline parameter values listed in Table 1, unless otherwise specified. We explore both scenarios: endemic equilibrium (EE) when $R_0 > 1$, and disease-free equilibrium (DFE) when $R_0 < 1$, examining the interplay between transmission dynamics and behavioral adoption of IKS practices.

The time-series plots in Figure 8 reveal a distinctive pattern: following epidemic onset, there is a rapid surge in the population of IKS adopters (V). This behavioral response to perceived disease risk creates a protective feedback that modulates subsequent transmission. Crucially, as demonstrated in Figure 5, the infectious compartment (I) exhibits delayed and attenuated peaks in scenarios with non-zero initial IKS adoption, compared to the case where adoption is absent ($x(0) = 0$). This illustrates the *curve-flattening* effect of culturally-grounded behavioral adaptation—a finding with direct relevance for outbreak mitigation strategies.

Further analysis shows that when the initial adoption rate is zero, the system can converge to an unstable endemic equilibrium even when $R_0 < 1$ (see Figure 5b), highlighting the role of initial conditions in bifurcation-driven dynamics. Conversely, for any non-zero initial adoption, the IKS adoption variable $x(t)$ tends asymptotically toward unity over time, irrespective of whether the disease persists or dies out (Figure 7). This indicates that once introduced, IKS practices can become self-sustaining within the population, driven by perceived benefits relative to costs. The stark contrast between $x(0) = 0$ and $x(0) > 0$ scenarios underscores a critical policy insight: seeding even minimal uptake of IKS practices among at-risk groups can catalyze long-term behavioral change, thereby enhancing community resilience against TB outbreaks.

In summary, these simulations confirm that the integration of IKS adoption dynamics substantially alters the epidemic trajectory, reducing peak prevalence, delaying outbreak peaks, and promoting convergence to lower endemic levels. The following subsections provide a detailed exploration of these dynamics, including bifurcation behavior, global stability under varying initial conditions, and the public health implications of the observed patterns. While the present simulations employ nationally averaged parameters, the model structure is amenable to **regional scenario analysis**. For instance, using state-level data from the India TB Report 2023 [16], one could parameterise the model separately for high-incidence states (e.g., Uttar Pradesh, Rajasthan) and low-incidence states (e.g., Kerala, Tamil Nadu). Such an exercise would reveal how regional variations in IKS adoption rates, treatment accessibility, and social mixing patterns influence epidemic trajectories and the effectiveness of behavioural interventions. Although not implemented here, this spatial stratification represents a natural and valuable extension for public health planning, enabling state-specific calibration of IKS promotion strategies.

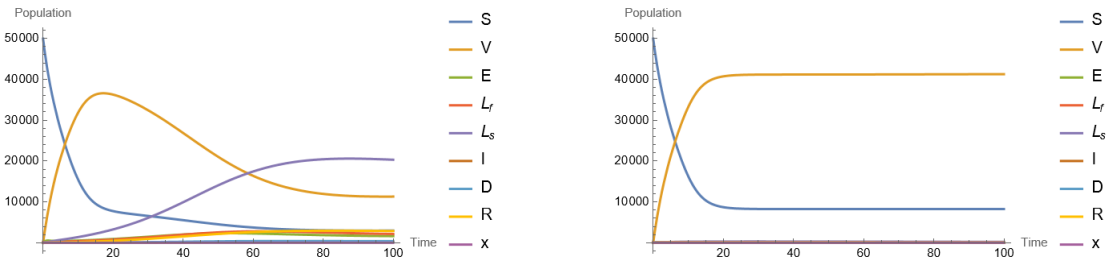

(a) (b)

Figure 4: Time series plot of the model in case of (a)$R_0 > 1$ (b) $R_0 < 1$

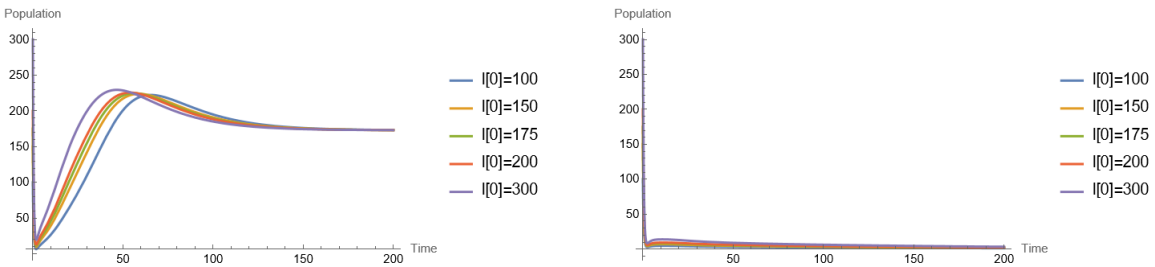

(a) (b)

Figure 5: Plot of Infectious Population with different initial seeding population for (a)$R_0 > 1$ (b) $R_0 < 1$

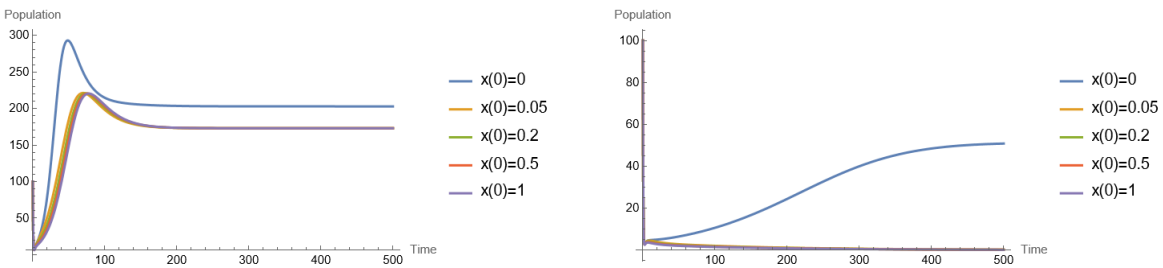

(a) (b)

Figure 6: Plot of Infectious Population with different initial IKS adoption rates for (a)$R_0 > 1$ (b) $R_0 < 1$

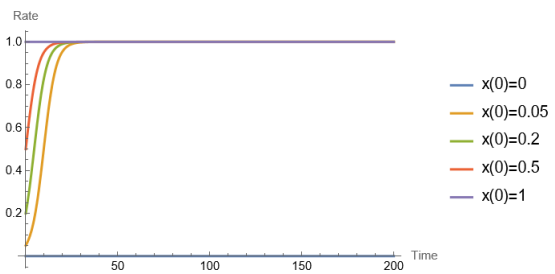

Figure 7: IKS Adoption rate over time

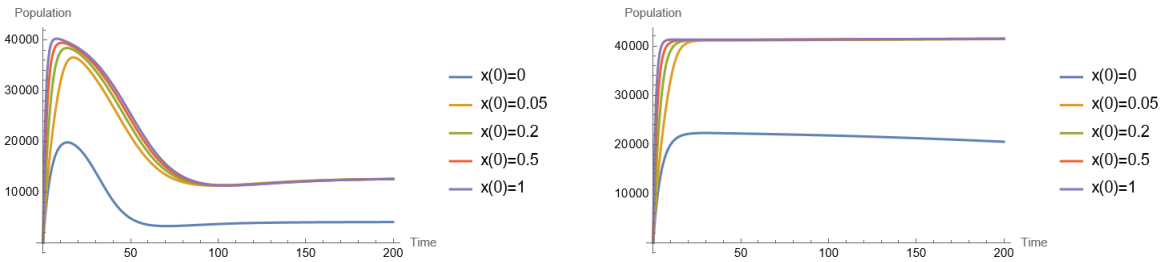

(a) (b)

Figure 8: Population of IKS Adoptors over time for (a)$R_0 > 1$ (b) $R_0 < 1$

Consistent with the analytical finding of backward bifurcation at $R_0 = 1$ (established in Section 5.4), Figure 9 illustrates this phenomenon numerically. The bifurcation diagram plots the equilibrium prevalence of active TB (I^*) against the basic reproduction number R_0, clearly showing the coexistence of stable endemic and disease-free branches for R_0 values below unity. This subcritical bifurcation indicates that reducing R_0 below 1 through conventional interventions may not suffice to eliminate TB if the system is trapped in the upper endemic branch—a result with direct implications for control policy design.

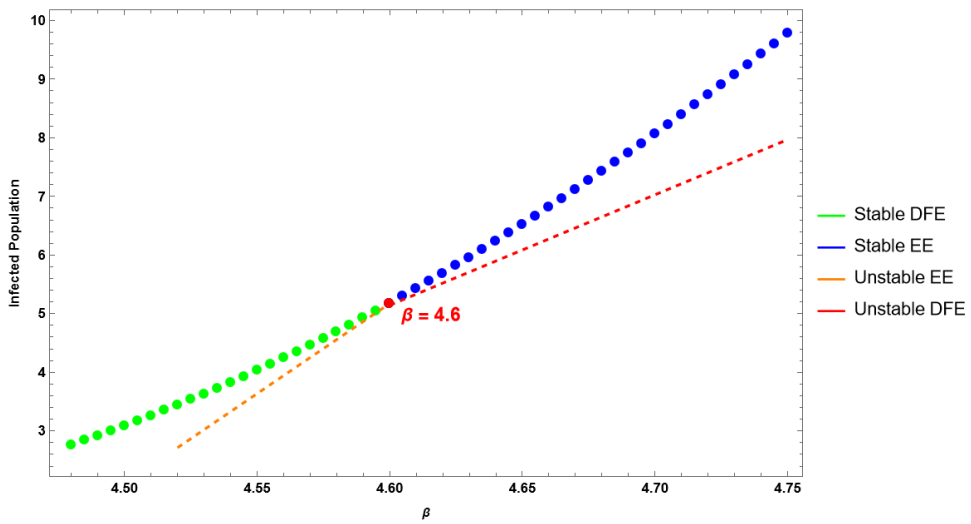

Figure 9: Bifurcation at $R_0 = 1$

7.1. Visualizing Global Stability

The global asymptotic stability of the endemic equilibrium is further corroborated through phase-space analysis. Figures presents parametric plots depicting trajectories from diverse initial conditions converging uniformly to the endemic equilibrium point. These visualizations confirm that, regardless of the starting state, all solution paths ultimately approach the same equilibrium, provided the initial IKS adoption rate $x(0)$ is consistently zero or consistently non-zero across compared scenarios. This observed convergence aligns with the Lyapunov stability proofs established in Section 5.5 and reinforces the robustness of the endemic equilibrium under the model's dynamics. The following panels illustrate this convergence behavior through projections in various three-dimensional subspaces of the state space, highlighting the invariant attracting nature of the endemic state.

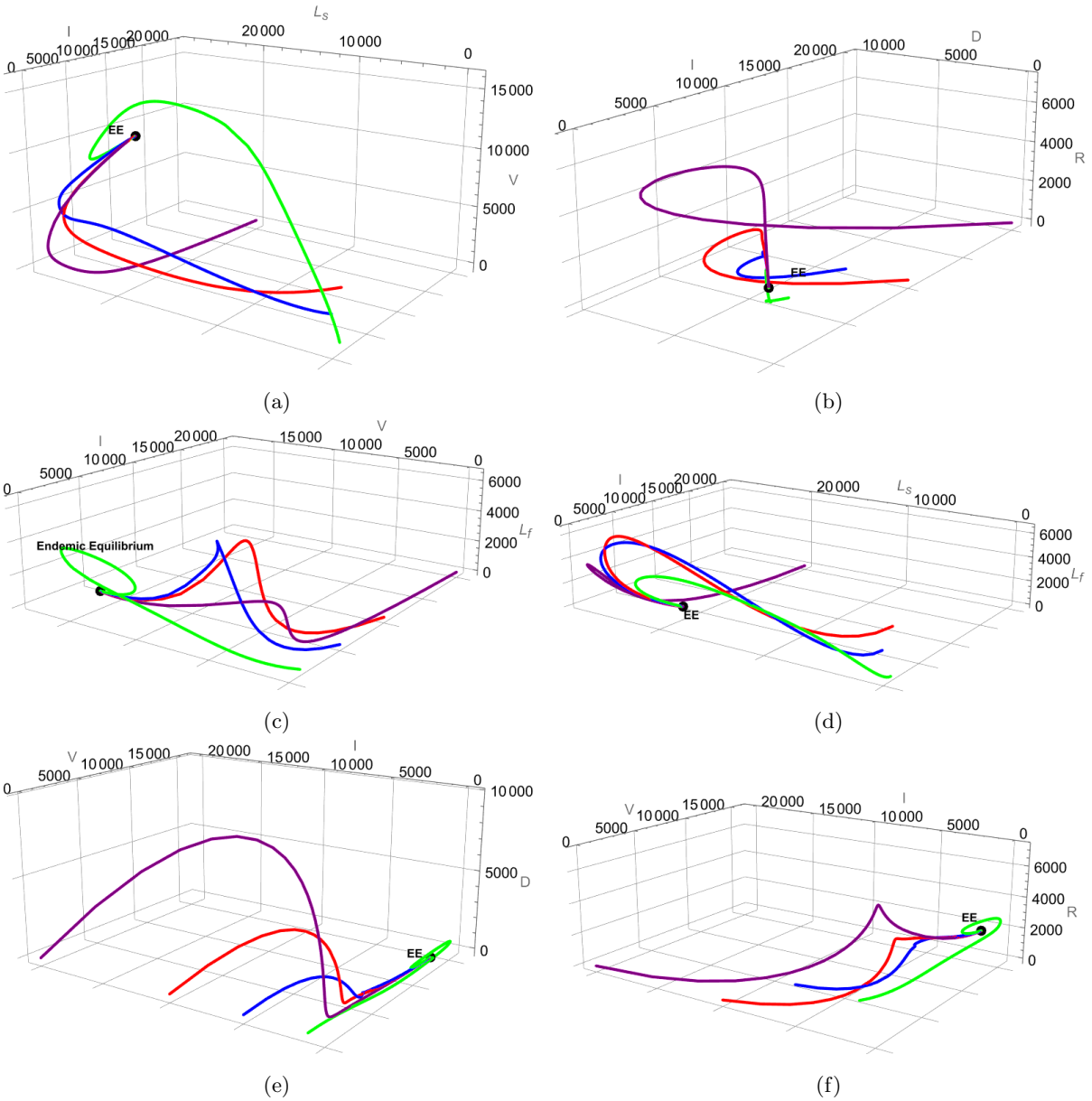

Figure 10: Global Stability of EE

8. Conclusion

This study has presented a pioneering mathematical framework that formally integrates principles from Indian Knowledge Systems (IKS) into the epidemiology of tuberculosis. By extending classical compartmental models with a dynamic behavioral adoption component, we have quantified the synergistic relationship between cultural health practices and disease transmission, establishing a novel paradigm for culturally contextualized public health modeling.

Our analysis yields several significant findings. First, the model demonstrates that IKS adoption, modeled as a logistic growth process influenced by perceived benefit and cost, creates a substantive feedback loop that meaningfully reduces the basic reproduction number R_0. The global stability results—proving that the disease-free equilibrium is stable when $R_0 < 1$ and the endemic equilibrium is stable when $R_0 > 1$—provide a robust mathematical foundation for policy planning. Notably, the identification of backward bifurcation at $R_0 = 1$ reveals an important epidemiological insight: even when R_0 is pushed

below unity through conventional interventions, a persistent endemic state may remain due to behavioral and cultural factors, necessitating integrated rather than siloed control strategies.

The sensitivity analysis further underscores the model's practical relevance. Parameters associated with IKS efficacy (ε_S) and adoption dynamics (μ_a, κ_a) emerged as key levers for reducing transmission, highlighting the potential of culturally-grounded behavioral interventions alongside biomedical measures. This aligns with the empirical context illustrated in Figure 1, which shows state-level TB notifications in India for 2020 and 2025. The observed decline in reported cases during this period must be interpreted with caution; as noted in co-infection studies, COVID-19 disrupted TB surveillance and healthcare access, likely leading to significant underreporting despite ongoing transmission. This reinforces the critical need for models that account for health system shocks and behavioral adaptations—precisely the gap our IKS-informed framework aims to fill.

Numerical simulations validate the theoretical predictions and demonstrate two key public health implications: (1) IKS adoption flattens the epidemic curve, delaying and reducing the peak prevalence of active TB, and (2) even moderate levels of sustained adoption can shift long-term dynamics toward lower endemic equilibria. These findings are not merely theoretical; they offer a quantitative basis for designing hybrid intervention programs that combine DOTS-based clinical care with community-driven, culturally resonant prevention.

In light of the heterogeneous burden shown in Figure 1—with high-prevalence states maintaining consistently elevated caseloads—our model also supports spatially targeted policy. Regions with entrenched TB transmission could benefit most from integrating IKS practices into local health campaigns, thereby addressing both biological and social determinants of disease. Furthermore, incorporating a geographical lens into the modelling framework underscores the importance of spatially targeted and culturally adaptive intervention designs. In a country as diverse as India, a one-size-fits-all approach to TB control is unlikely to succeed. Instead, policies should be informed by regional epidemiological profiles and cultural landscapes, aligning IKS promotion with local health narratives and community infrastructures. Future research could extend this model into a spatially explicit or meta-population framework, incorporating migration networks, urban–rural gradients, and state-level heterogeneity in transmission and behaviour. Such advancements would not only enhance the model's realism but also provide a scalable template for integrating indigenous knowledge systems into geographically informed public health strategy.

Ultimately, this work bridges a persistent gap between traditional knowledge and modern computational epidemiology. It moves beyond anecdotal or qualitative appreciation of IKS by providing a rigorous, dynamical systems-based tool to simulate, evaluate, and optimize culturally informed TB control strategies. As global health moves toward more inclusive and context-aware frameworks, the methodology developed here offers a replicable template for integrating indigenous knowledge systems into infectious disease modeling—not only for TB in India, but for a wide range of settings where culture and health are deeply intertwined.

Future work will focus on calibrating the model with longitudinal adoption data, exploring optimal control strategies that leverage IKS practices alongside vaccination and treatment, and extending the framework to co-infection scenarios with HIV or COVID-19. By continuing to refine this synergy between traditional wisdom and mathematical rigor, we can build more resilient, equitable, and effective public health responses for the world's most persistent infectious diseases.

References

1. Tiemersma, E. W., van der Werf, M. J., Borgdorff, M. W., Williams, B. G., & Nagelkerke, N. J., *Natural history of tuberculosis: duration and fatality of untreated pulmonary tuberculosis in HIV negative patients: a systematic review*, PLoS ONE 6(4), e17601, (2011).

2. Salje, H., Cummings, D. A., & Lessler, J., *Estimating infectious disease transmission distances using the overall distribution of cases*, Epidemics 7, 1-8, (2014).

3. Vynnycky, E., & Fine, P. E., *The natural history of tuberculosis: the implications of age-dependent risks of disease and the role of reinfection*, Epidemiol Infect 119(2), 183-201, (1997).

4. Sutherland, I., Svandová, E., & Radhakrishna, S., *The development of clinical tuberculosis following infection with tubercle bacilli. 1. A theoretical model for the development of clinical tuberculosis following infection, linking from data on the risk of tuberculosis infection and the incidence of clinical tuberculosis in the Netherlands*, Tubercle 63(4), 255-268, (1982).

5. Menzies, N. A., Cohen, T., Lin, H. H., Murray, M., & Salomon, J. A., *Population health impact and cost-effectiveness of tuberculosis diagnosis with Xpert MTB/RIF: a dynamic simulation and economic evaluation*, PLoS Med 9(11), e1001344, (2009).

6. Castillo-Chavez, C., & Song, B. (2004).*Dynamical models of tuberculosis and their applications* . Mathematical Biosciences and Engineering, 1(2), 361-404.

7. Styblo, K., *Epidemiology of tuberculosis*, Selected Papers 24, 1-104, (1991).

8. Office of the Registrar General & Census Commissioner, India, *Sample Registration System Statistical Report 2021*, Ministry of Home Affairs, Government of India, (2023).

9. Central TB Division, Ministry of Health and Family Welfare, *India TB Report 2023*, Government of India, (2023).

10. World Health Organization, *Global Tuberculosis Report 2023*, World Health Organization, (2023).

11. Central TB Division, *TB Mortality in India: Analysis of Vital Registration Data*, Ministry of Health and Family Welfare, Government of India, (2023).

12. Zwerling, A., Behr, M. A., Verma, A., Brewer, T. F., Menzies, D., & Pai, M., *The BCG World Atlas: a database of global BCG vaccination policies and practices*, PLoS Med 8(3), e1001012, (2011).

13. Andrews, J. R., Noubary, F., Walensky, R. P., Cerda, R., Losina, E., & Horsburgh, C. R., *Risk of progression to active tuberculosis following reinfection with Mycobacterium tuberculosis*, Clin Infect Dis 54(6), 784-791, (2012).

14. India Tuberculosis Profile, World Health Organization, (2023). Available at: https://worldhealthorg.shinyapps.io/tb_profiles/.

15. Verma, V. S., Kaushik, H., & Bhadauria, A. S., *Mathematical modelling of tuberculosis and COVID-19 co-infection in India: a real data analysis on concomitant diseases*, Appl Appl Math 18(1), (2023).

16. Central TB Division, Ministry of Health and Family Welfare, *India TB Report 2023*, Government of India, (2023).

[3] *University of Allahabad, Prayagraj, India.*

E-mail address: ruchikasingh.geo@gmail.com